Chapter 2

Glass and Glass-Ceramic Scaffolds: Manufacturing Methods and the Impact of Crystallization on *In-Vitro* Dissolution

Amy Nommeots-Nomm and Jonathan Massera

Additional information is available at the end of the chapter

http://dx.doi.org/10.5772/intechopen.70242

Abstract

Synthetic biomaterials mimicking bone morphology have expanded at a tremendous rate. Among all, one stands out: bioactive glass. Bioactive glasses opened the door to a new genre of research into materials able to promote the regeneration of functioning bone tissue. However, despite their ability to promote cell attachment, proliferation and differentiation, these materials are mainly used as granules. However to promote loaded and sustained bone repair, a 3D structure, with open and highly interconnected pores, is desirable. 3D scaffolds are generally produced into green bodies via various techniques. The particles are then bound together via sintering. However, the highly disrupted silica network of the typical bioactive glasses composition leads to crystallization. Therefore, sintering of the most commonly used bioactive glass compositions (i.e. 45S5 and S53P4) leads to partly to fully crystallize bodies. The impact of crystallization on bioactivity still leads to large debate among the scientific community. Does crystallization reduce or suppress the materials bioactivity? Within this chapter, the processing routes for scaffold manufacture are presented, as well as an introduction to the thermal processing of glasses to form glass and glass-ceramics and the consequent effect on bioactivity is discussed.

Keywords: scaffold, bioactive glass, crystallization, glass-ceramic, *in-vitro* dissolution

1. Introduction

With the ageing and continuous growth of the population, surgeons face an increasing number of operations aiming to replace and/or repair tissue that has been damaged through disease and trauma [1]. According to the International Osteoporosis Foundation,

incidence of fracture, for example, is anticipated to increase by 240% in women and 310% in men by 2050 [http://www.mdbuyline.com/research-library/articles/bone-graft-substitutes-bone-matrix-cost/, visited last April 2016]. This factor is expected to drive the rise in the global bone graft market. Bone regeneration market was evaluated at USD 2.35 billion in 2014 and is expected to rise to USD 3.48 billion by 2023, as reported in transparency market research [http://www.transparencymarketresearch.com/pressrelease/bone-grafts-substitutes-market.htm, visited June 2017]. The gold standard in bone grafts is, at present, the use of allograft. An allograft is a tissue received from a donor which is demineralised before use, thus, genetically different than an autograft (where tissue comes from the patient itself). However, a risk of infection is associated with such practices. To overcome the infection risk, the allograft tissue must be pre-treated. Techniques used are tissue freezing, freeze drying and sterilization. The average cost per procedure was estimated to be USD 3154.

Bioceramics, pertaining to their excellent biocompatibility and higher mechanical properties compared to polymers or metals, have always been regarded as the most promising biomaterials for hard tissue repair. The advantage of bioceramics lies in their wide tissue/implant response: from being nearly inert to bioactive depending on their composition. A subset of bioceramics which have expanded at a tremendous rate in the past decade are bioactive glasses. These materials support not only osteoconduction (growth of bony tissue at the surface of the implant) but also osteoinduction (acceleration of new bone formation by chemical means) [2]. Bioactive glasses have, now, been used widely clinically especially in dental and bone repair applications.

For the repair and regeneration of bone defects, tissue engineering strives to produce 3D constructs that can support mechanical load and provide a template in which cells can migrate and colonized. The optimum attribute of a 3D scaffolds are summarized as follow:

- The biomaterials should not only be biocompatible but must support cell adhesion and proliferation. The material should be at minimum osteoconductive but ideally osteoinductive.
- The biomaterials should resorb over time. The resorption rate of the implant should match as closely as possible the regrowth of the new tissue.
- The implant should be porous with an open interconnect structure to allow fluid penetration, angiogenesis and cell proliferation. In general, interconnected pores of at least 100 μm and an open porosity of over 50% is considered the minimum requirement for tissue ingrowth [3-5]. Optimally, it is reported that the construct should have pores within 100–500 μm and an overall porosity of over 90%. However an increase of porosity comes at the expense of mechanical strength [6].
- The mechanical properties, which is mainly function of the porosity and the pores organisation, should be tailored to the site of implantation, i.e. similar to cancellous bone in non-load bearing applications and similar to cortical bone in load-bearing applications. In all case, the mechanical properties should be maintained throughout the bone reconstruction.

http://dx.doi.org/10.5772/intechopen.70242

2. Scaffold fabrication

2.1. Foamed morphology processing

2.1.1. Porogen

Porogen processing is a method in which glass powders are mixed with a polymer bead used as a 'space holder', and packed into a mould. The polymer is then burnt away in a two stage sintering process to create porous scaffold. This process relies on using a combustable polymer and sufficient oxygen flow to gain complete burn out during sintering, if complete burn out is not achieved it can result in inhomogeneous scaffolds being formed with a porosity gradient. The scaffolds tend to have limited porosity of up to 50% [7].

2.1.2. Freeze casting

Freeze casting is a traditional ceramic foam processing method, which is based upon the formation of an aqueous slurry where ice crystals are formed in the direction of freezing. Under vacuum, the ice crystals are then sublimated to leave a porous green body which is then sintered [8]. This was initially developed in 2011 for use with hydroxyapatite, but has since been used with various glass and glass-ceramic compositions [9-11]. The scaffolds produced tend to have small pores (up to 100 μm) with low levels of interconnection, with consequently high strengths. Due to the small pores, they have not been significantly investigated in either the glass or glass-ceramic field for bone repair.

2.1.3. Foam replica process

The foam replica process employs a polymeric foam, commonly made of polyurethane, to act as a template for a glass slurry to create scaffolds with a foamed morphology. The foam is soaked in a glass suspension, and dried. By completing multiple cycles of infiltration and drying the wall thickness of the scaffolds can be increased, however, the shape obtained is still dependent upon the foam itself. The sintering process is then completed in two stages, firstly to burn out the polymer foam, and secondly to sinter the particles to form a continuous construct. The foam template is key within this process, its pore shape, size, and distribution all control the outcome of the scaffolds produced. The mechanical properties of the scaffolds produced via this technique are predominately dependent upon the particle distribution within the foam prior to burnout, which is controlled by the stability and concentration of the suspension used.

The process was first adopted to produce glass ceramics from the 45S5 composition in 2006. Scaffolds were produced from 45S5 glass powder, then sintered at 1000°C for 1 hour, forming fine crystals of $Na_2Ca_2Si_3O$ [12]. It was then adapted by Fu et al. [13] using the 13-93 glass composition which were kept amorphous post sintering (54.6 SiO_2, 22.4 CaO, 6 Na_2O, 1.7 P_2O_5, 7.9 K_2O, 7.7 MgO in mol%). The scaffolds met many of the requirements for bone regeneration, with a reported porosity of 85 ± 2%, interconnected pores between 100 and 500 μm, and compressive strengths of 11 ± 1 MPa. These values are similar to those of human trabecular

bone and outperformed other glass-ceramic foams reported in literature at the time [13]. This could be attributed to their optimisation of glass loading within the slurry. Their particle size distribution (modal size of 2 μm) allowed for good particle packing within the green body enhancing sintering. Combining this with the sintering window provided by the 13-93 composition allowing viscous flow without crystallisation during sintering, leads to the formation of dense struts with limited distortion of the foams morphology.

Table 1 summarises the variety of glass and glass ceramics that have been produced via this method; as shown there are large differences between the properties obtained but it highlights the flexibility of the processing method. A limitation of the foam replica process is that excess slurry can become trapped inside the sacrificial polymer foam after infiltration, which can be difficult to remove prior to burnout and sintering. It has to be squeezed out and if excess slurry remains, the structure produced will be heterogeneous with a porosity gradient being formed. Even with optimum processing, the foam replica method can leave struts with hollow centres which reduce the mechanical properties and performance of the scaffolds [14].

2.1.4. Gel-cast foaming

Sepulveda and Binner [15] first used gel-cast foaming to create porous ceramics. Rather than using a foam template, as used within the foam replica process, the ceramic slurry was foamed under vigorous agitation with the aid of a surfactant. The process used in-situ polymerisation of an organic monomer, such as methacrylamide, to form a gel and stabilise the foam. The polymer was then burnt out during the sintering cycle. Wu et al. [16] adapted this gel-casting process to manufacture scaffolds using the composition ICIE16 (49.46% SiO_2, 36.27% CaO, 6.6% Na_2O, 1.07% P_2O_5 and 6.6% K_2O, in mol%). The process was based upon in situ polymerisation of acrylamide by using a cross-linker, surfactant and initiator. Although this alternative processing method avoided the 'hollow strut' issues associated with the foam replica process it was limited in its ability to be scaled up to higher volume manufacture due to the small gelation window of the polymer used, it was also shown to precipitate sulphur rich crystals upon the glass surface. The scaffolds produced by Wu et al. [16] had porosities of 79%, with modal pore diameters of 379 μm and compressive strength of 1.9 MPa. These values were a factor of 10 lower than those reported by Fu et al. for foam replica scaffolds manufactured from 13-93 [13].

The gel-casting process was later adapted by Nommeots-Nomm et al. by using the thermally controlled gelation of gelatin to increase the processability of the system and stop unwanted sulphur byproducts. Amorphous scaffolds with foam morphologies were produced with porosities of 75% with modal pore interconnects between 100 and 150 μm. Scaffolds were produced from three glass compositions ICIE16, PSrBG (44.5 SiO_2, 17.8 CaO, 4 Na_2O, 4.5 P_2O_5, 4 K_2O, 7.5 MgO and 17.8 SrO mol%) and 13-93 with compressive strengths of 3.4 ± 0.3, 8.4 ± 0.8 and 15.3 ± 1.8 MPa respectively, higher than values presented in literature for equivalent foamed scaffolds. *In-vivo* analysis within a femoral head defect in a rabbit model supported growth across 12 weeks; however, the rate of scaffold degradation raised some questions about its suitability for a human model [26].

This process has also been adapted for the production of glass ceramics and more recently glass ceramics from pre-ceramic polymers. Fiocco et al. used pre-ceramic polymers to produce wollastonite diopside scaffolds with 77% open porosity and compressive strengths of 1.8 ± 0.3 MPa [27].

Composition name	Composition used/ mol %	Pore size/μm	Porosity/%	Compressive strength/MPa	Reported bioactivity
Glass-ceramics					
CEL2 [17]	45% SiO_2, 3% P_2O_5, 26% CaO, 7% MgO, 15% Na_2O, 4% K_2O	100–300	75	1 ± 0.4	HA reported after 1 week
Borosilicate® [18]	P_2O_5–Na_2O–CaO–SiO_2	200–500	95	0.06 ± 0.01	HA reported after with 72 hours
[19]	57SiO_2–34CaO–6Na_2O–3Al_2O_3 crystal formation: $CaSiO_3$	Mean: 240	56 ± 6	18	Not reported
45S5 [12]	Crystallised phase: $Na_2Ca_2Si_3O_9$	510–720	89–92	0.27–0.42	HA reported after 3 days
45S5 [20]	Crystallised phase: $Na_2Ca_2Si_3O_9$	Not reported	90	0.4	Not tested
45S5 [21]	$Na_6Ca_3Si_6O_{18}$ and $Na_2Ca_4(PO_4)_2SiO_4$	25–600	61 ± 3	13.78 ± 2.43	HA reported after 7 days
Glass					
Zn-doped borosilicate [22]	6Na_2O, 8K_2O, 8MgO, 22CaO, 36B_2O_3, 18SiO_2, 2P_2O_5; Zn substitution at 1.5, 5 and 10 wt.% ZnO	200–400	80–92 ± 7	Not reported	HA reported after 90 days,8 weeks in a rat calvarial defects, glass doped with 5% Zn enhanced bone formation
13-93 doped with copper [23]	6Na_2O, 8K_2O, 8MgO, 22CaO, 36B_2O_3, 18SiO_2, and 2P_2O_3 (mol%) Copper doping at 0, 1 and 3 wt.%	100–300	85 ± 3	Not reported	HA reported after 90 days
13-93 doped with cobalt [14]	wt.%: 53SiO_2, 6Na_2O, 12K_2O, 5MgO, 20CaO, and 4P_2O_5 Cobalt doping at 0 wt.%, 1 wt.% and 5 wt.% CoO	200–400	89–91	2.3–4.2	HA reported after 3 days
13-93 [13]	53SiO_2, 6Na_2O, 12K_2O, 5MgO, CaO, 4P_2O_5 wt.%	100–500	85 ± 2	11 ± 1	Within 7 days
13-93B1 [24]	6% Na_2O, 8% K_2O, 8% MgO, 22% CaO, 18% B_2O_3, 36% SiO_2, 2% P_2O_5	Mean 500	78	5.1 ± 1.7	HCA within 30 days, to non critical osseous defect model in a rabbit, one in the femoral head, one in radius bone supported regrowth
[25]	22 CaO, 6 Na_2O, 8 MgO, 8 K_2O, 18 SiO_2, 36 B_2O_3, and 2 P_2O_5	250–500	72 ± 3	6.4 ± 0.1	HA reported after 7 days

Table 1. Summary of the glass and glass-ceramic scaffolds reported in literature produced via the foam replica method.

2.2. Additive manufacturing techniques

2.2.1. Selective laser sintering

Selective laser sintering (SLS) is a layer-by-layer additive manufacture technique capable of manufacturing green bodies. Glass particles are most commonly mixed with a thermoplastic binder after which, a laser locally heats the areas of interest creating a layered green body, the powder bed then drops down and another layer of particulate is dispersed and then selectively bound. Unbound particles are removed and the green body is sintered using a two stage process to remove the binder and merge the particles together. As with most powder based 3D printing technique, its advantages are that complex or challenging geometries can be manufactured. However, it is limited by the accuracy of the laser, the size of construct that can be produced, the detail of the features that can be formed, and the ability to completely burn out the binder without leaving residual porosity [28].

One study utilising SLS by Velez et al. reports scaffolds of 13-93 glass, with particles of sizes up to 75 μm, using stearic acid as a binding agent. The scaffold with 50% porosity had strengths of 40 ± 10 MPa post-sintering [29]. Work by Kolan et al. [28] reported mechanical properties within the same range as Velez et al. [29] of 41 MPa for 50% porosity. Their work looked at optimising the process by reducing the binder concentration and particle size, and increasing the laser power to increase processing speed. However, the time to produce scaffolds compared with competing 3D printing techniques, such as direct ink writing was still much longer.

2.2.2. Stereolithography

Stereolithography is a slurry-based 3D printing technique; a bed is flooded with a homogenous dispersed slurry of particles containing a photocurable polymer. A laser is then used to cure the polymer locally to build a layer of the desired design. The bed is then dropped down and flood again with the slurry, and a second layer is cured into place. The stereolithography process offers the freedom to design and fabricate very complex shapes, but again as with selective laser sintering the processing times are slow.

45S5 glass-ceramic scaffolds have been successfully printed into a variety of pore design and geometries [30]. They found that, for a diamond-like structure, reducing the pore size from 700 to 400 μm while maintaining the same overall porosity (~60 vol%) increased the mechanical strength from 3.5 to 6.7 MPa respectively.

2.2.3. Robocasting

Robocasting is another '3D printing' method being used to manufacture porous scaffolds from bioactive glasses. Originally developed in 1998 by Cesarano et al., it can be described as a solution based extrusion process controlled by computer aided design [31]. The robocasting technique relies on the formulation of glass loaded inks which can be extruded through fine diameter nozzles. An example of the scaffolds produced is shown in **Figure 1**. The first development of this technique relied on manipulating the interparticle forces within particle loaded suspensions to create inks with the correct rheological properties for printing [31]. Now binder 'inks' are formulated with the correct rheological properties to act as a carrier of

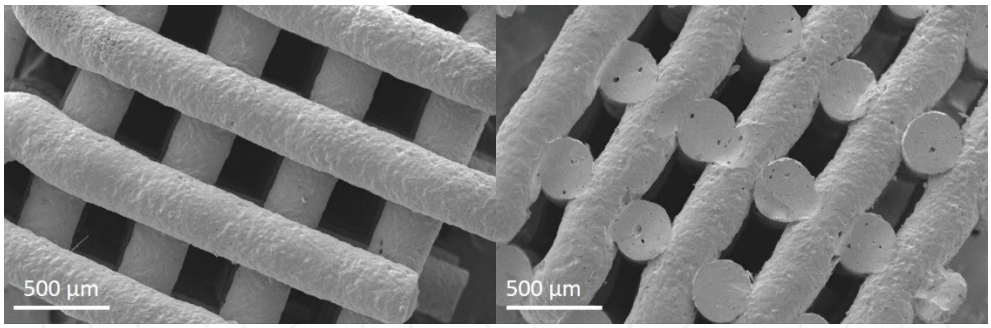

Figure 1. An example of robocast scaffolds produced from ICIE16 bioactive glass (authors own).

the particles which bind them together prior to sintering. An ideal ink would be easy to mix, allow for high glass powder loadings while maintaining a printable viscosity, have pseudoplastic rheological properties, and yield strength and storage modulus high enough to be able to withstand the weight of multiple layers of scaffolds and the spanning distance.

Robocasting is the most commonly used 3D printing technique for bioactive glasses. This is for a number of reasons: the speed of fabrication; the ease at which inks can be produced; and the capability and accessibility of the machines. This enables the printing of inks with high glass loading, which produce scaffolds with low strut porosity, enhancing their mechanical properties.

The first robocasting paper published from a bioactive glass was by Fu et al. using 13-93 glass and Pluronic F-127 surfactant as a carrier ink [32]. Pluronic F-127 is a block co-polymer surfactant with thermally reversing rheological behaviour, made up of poly(ethylene oxide)-poly(propylene oxide)-poly(ethyleneoxide) tri-blocks (PEO-PPO-PEO) ($HO(C_2H_4O)a(C_3H_6O)b(C_2H_4O)c$). Pluronic F-127 can be dissolved in water, forming a stable suspension via steric repulsion of the –OH groups [33-35]. Due to its thermally reversible properties it enables easy mixing of glass particle at low temperatures while enabling the formation of high modulus, and high stiffness pseudoplastic inks at room temperature. Since Fu's initial work, groups have worked with a variety of different glass and binder chemistries, summarised in **Table 2**.

Glass used	Max glass loading/vol %	Ink chemistry and (dispersant)	Strut size/µm	Pore size/µm	Porosity/%	Compressive strengths/MPa
6P53B [32]	30	F-127 (water)	100	500	60	136 ± 22
13-93B3 13-93 [38]	45	Ethyl cellulose/PEG (ethanol)	300 ± 20	420 ± 30	48 ± 3	65 ± 11 142 ± 20
13-93 [39]	40	F-127 (water)	330	300	47	86.9 ± 9
45S5 [40, 41]*	45	Carboxymethyl cellulose (water)	250–300**	Not available	63 ± 3	13 ± 1

*Not amorphous post sintering.

**Values not reported, therefore, measured using imageJ from the published SEM images available.

Table 2. Summary of current literature on scaffolds produced via direct ink writing.

The homogeneity of the ink, particle packing, sintering process, strut size and spacing all contribute to the scaffolds overall mechanical properties. Due to the periodically arrange structure the strengths achieved are substantially higher than other scaffold processing methods, offering strengths in the range of cortical bone instead of cancellous [36].

Glass-ceramic scaffolds have also been produced via this technique. Roohani-Esfahani et al. produced scaffolds of various designs from a heat treated sol-gel Sr doped $Ca_2ZnSi_2O_7$ (HT) composition. They reported high strengths in excess of 100 MPa with high fatigue and crack resistance created by the multiphase composition [37].

3. Sintering and crystallization

One point, that all scaffold processing technique have in common, is the necessity for a sintering step. Sintering is a thermally induced phenomenon where, initially, the particles will undergo viscous flow. Viscous flow will ultimately lead to reorientation of the glass particles and neck growth. At a later stage, the contact between particles will grow and the pores will shrink resulting in a dense body where, usually, some closed pores will become trapped. Trapped pores are characteristically in the sub-micron range. However, in the case of glass and more particularly bioactive glasses, the heating process may induce crystallization.

The crystallization of the two most used and FDA approved glass, i.e. 45S5 and S53P4, has been studied in details by Massera et al. [42]. In this study, the activation energy for viscous flow as well as the activation energy for crystallization was quantify for fine (<45 μm) and coarse (300–500 μm) glass particles. As expected, the activation energy for viscous flow was independent of the glass particle size and ranged between 750 and 800 kJ/mol. On the other hand, the activation energy (Ec) for crystallization was found to be constant with respect to glass particles size, for the glass S53P4 with a value around 300 kJ/mol. In the case of the glass 45S5, Ec was found to decrease, from 338 to 230 kJ/mol, with increasing particles size. This is typically an indication of a change in the crystallization dimensionality with respect to the crystal size. The Jonhson-Mehl-Avrami exponent, which gives an indication of the dimensionality of the primary crystal phase, was calculated. While a value of ~1 was constantly derived for the glass S53P4, independently of the technique used (Augis and Bennett equation, Ozawa and isochronal method), the value was found to change from 0.8 to 2.8 when using the Augis and Bennett equation. Not only the 'n' exponent was found to change as a function of particles size but it also varied depending on the method employed. Such variation in the JMA exponent calls for questioning the Johnson-Mehl-Avrami crystallization model. The JMA model validity was tested using the methods proposed by Malek and Mitsuhashi [43]. While the JMA model was validated for the glass S53P4, the JMA model was found to be unsuitable to the crystallization of glass 45S5. Overall, both glass S53P4 and 45S5 were found to be fragile glass, i.e. a small change in temperature leads to a significant change in viscosity. The activation energy for viscous flow is high indicating that sintering or fibre drawing at moderate temperature will be virtually impossible. Crystallization is surface initiated (n ~ 1) for the glass S53P4. **Figure 2a** presents a SEM image of the glass surface after a heat treatment at 730°C for 2 hours and **Figure 2b** presents the crystallized layer thickness as a function of heat treatment time.

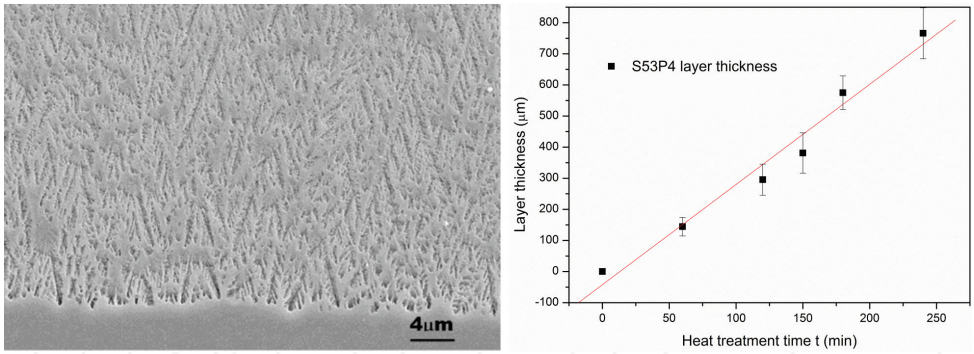

Figure 2. SEM image of a glass S53P4 heat treated for 2 hours at 730°C (a) and layer thickness as a function of heat treatment time at 730°C (b) (authors own).

As shown in the SEM image the crystallization initiates at the glass surface with a growth rate of about 3.5 μm/min. Such crystallization kinetic will prevent proper sintering of the glass particles. Furthermore, one should keep in mind that during scaffolds processing, it is generally accepted, that small particles size should be used. Decreasing the particles size leads in an increase in the surface area and therefore an increase in nucleation sites. Therefore, this glass may not be suited for the sintering of amorphous scaffolds.

The crystallization of the glass 45S5, described in [42] seemed to be initiated within the bulk. However, it appears that the glass becomes phase separated, with one amorphous phase crystallizing at lower temperatures than the secondary phase. Upon increasing the duration of the heat treatment the crystals grew via surface controlled crystallization thereby the elements of the secondary phase, at the interface with the crystals, 'feeds' the crystal. The formation of large pores was also evident during sintering of this glass composition.

The kinetics driving the crystallization of the two most known and clinically used bioactive glasses does not permit complete sintering of scaffolds without formation of crystallites.

4. Impact of crystallization on bioactivity

The impact of crystallization on the bioactivity or, more precisely, on the ability of the glass to precipitate a HA layer, has been first studied by Peitl Filho et al. [44]. Their conclusion was that below 60% crystallinity the ability of the glass 45S5 to precipitate a reactive layer was not impaired whereas above 60% crystallinity the reactive layer precipitated at a slower rate. This was then confirmed with glass S53P4 by Fagerlund et al. [45]. They demonstrated that when the glass particles were heat treated at temperature to maintain the glass fully amorphous a clear formation of Si-rich layer, a mixed layer and a Ca–P with a Ca/P = 1.6–1.7 was formed. When the glass started to crystallize, the precipitated reactive layer was much thinner and disappeared with an increase in heat treatment temperature. Interestingly, at temperature above 750°C a secondary crystal phase was formed. Upon immersion in simulated body fluid the primary crystal

phase, belonging to the combeite composition dissolved, leading to the formation of thick mixed-layer. However, no Ca–P reactive layer precipitated at the surface of the particles. Furthermore, the secondary phase was found insoluble in simulated body fluid. Therefore, it can be concluded that while the bioactivity is not fully suppressed in this silicate-bioactive glasses a clear decease in the ability of the glass to form a HA layer was greatly slowed down. One should keep in mind that the precipitation of such layer is only a small contribution of the glass towards the bioactivity and, as such, is not sufficient to make firm conclusion regarding the bioactivity of the materials *in-vivo*. Nonetheless, it remains that one of the most interesting aspects of bioactive glasses is the release of therapeutic ions in a control fashion and this cannot be controlled when the glass is crystallized in an uncontrolled manner, as it is the case during sintering of rapidly crystallizing glasses. Such uncontrolled crystallization also raises the question about the ability to confidently reproduce similar microstructure, which would be key in production for the clinic.

Other well-known and promising bioactive glasses for bone regeneration belongs to the phosphate composition. Ahmed et al. [46] Neel et al. [47], as well as Massera et al. [48–50], have developed phosphate glass composition that not only can promote cell attachment and proliferation but that can also be shaped into fibres. Nevertheless, a thorough understanding of the glass crystallization is necessary in order to understand the possibilities and limitations of these glasses. Massera et al., developed a glass within the $50P_2O_5$–$(40–x)CaO–xSrO–10Na_2O$ that can promote the activity of human gingival fibroblasts [49]. The crystallization kinetics of these glasses along with the *in-vitro* dissolution in simulated body fluid of partially to fully crystallized glasses has been studied in [50]. If heat treated at temperature below their crystallization, the reactive layer precipitation rate remained unchanged. Particles that were partially crystallized were ground to 125–250 μm particles size. The crystallization was found to initiate at the surface of the glass particles. During the grinding process the particles were fractured and revealed surfaces that were crystallized and some surfaces that were amorphous. **Figure 3** shows the SEM image of crushed glass particles with an amorphous surface and a rounded crystallized surface after 72 hours of immersion in simulated body fluid.

Figure 3. SEM micrograph of glass with composition $50P_2O_5$–$20CaO–20SrO–10Na_2O$ heat treated at 40°C below the crystallization temperature Tp (from DTA) for 30 min and immersed for 72 hours in simulated body fluid (reproduced from Massera et al. [49] with permission).

It appears clear on the SEM micrographs that the precipitation of the reactive layer is not suppressed. However, the reactive layer is only visible at the amorphous surface. This indicates that fully crystallized phosphate glasses will not support the precipitation of reactive layer.

A fully crystallized phosphate glass ($50P_2O_5$–$40CaO$–$10Na_2O$) was also immersed in simulated body fluids. No reactive layer could be detected at the surface of the glass particles. The phosphate and calcium ions released within the solution were quantified by ICP and are presented in **Figure 4**.

As expected the amorphous glass released phosphate ions and consume the calcium. This is attributed to the congruent dissolution of the phosphate glass and subsequent precipitation of a calcium phosphate reactive layer with a Ca/P ratio of 1. The crystallized glass, however, released a greater amount of P whereas the Ca remained constant within the accuracy of the measurements. From XRD the fully crystallized glass is composed of $NaCa(PO_3)_3$ crystals and $Ca(PO_3)_2$. The $NaCa(PO_3)_3$ crystals which is the primary crystal phase is more soluble than the secondary phase. The large release of phosphorus ions leads to a drastic decrease in the pH, which suppress the precipitation of the reactive layer [50].

Therefore, one can say that the impact of crystallization on the *in-vitro* dissolution can either reduce or suppress the precipitation of the CaP reactive layer. Also, one should keep in mind that the ion release of the partially to fully crystallized glass will be different than the original amorphous composition. The impact of crystallization on the bioactivity is a function of the crystal composition, crystal density and the composition of the remaining amorphous phase.

Alternative composition, which can be processed into amorphous porous scaffolds, are available. One example, among others, is the glass 13-93 [51]. This glass has been found to be bioactive and to have a wide hot forming window and a viscosity/temperature relationship enabling sintering prior to the crystallization. More recently, another family of glass composition which is gaining interest are borosilicate. Fu et al., taken as an example, processed 13-93 glass composition were the SiO_2 was partially to fully replaced by B_2O_3 [52]. They demonstrated that the

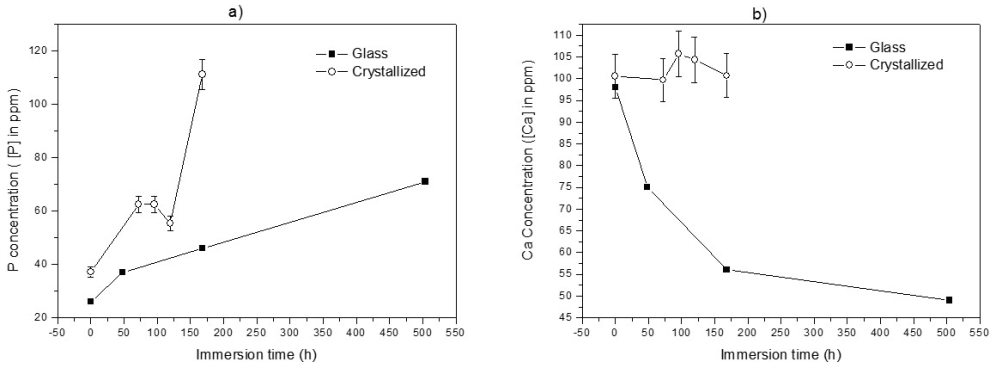

Figure 4. [P] (a) and [Ca] (b) concentration in the simulated body fluid when the glass and the corresponding crystallized are immersed for various times (authors own).

precipitation of the hydroxyapatite was accelerated with the presence of boron. However, the cell proliferation, *in-vitro*, was greatly reduced both in static and dynamic test. Nevertheless, the *in-vivo* outcome of these materials was positive [52]. Other researcher are attempting to develop borosilicate glass based on the fast dissolving bioactive 45S5 and S53P4 [53].

5. Conclusion

The current need for an off the shelf bone repair product is evident, and due to the current ageing demographic that need is growing. Literature presents a wide variety of bioactive glass and glass-ceramic compositions with tailored bioactivity and therapeutic effects suitable for bone repair. A huge wealth of different scaffold processing methods have been employed in the last 10 years, offering different morphologies, porosities and mechanical strengths. Previously these materials have been limited by their mechanical strength - porosity relationships. However, since 2011, with the growth of 3D printing, scaffolds with compressive strengths in the range of cortical bone have now been developed.

The common point of all scaffolds processing technique is the need for a sintering step at medium to elevated temperature. Sintering of bioactive glass is known to often lead to glass crystallization. Understanding the relationship between crystallization and bioactivity of bioactive glasses is of paramount importance. The available results demonstrate that the impact of the crystallization can have various effect on bioactivity depending upon the glass composition in question. While partial to full crystallization of the most known and widely used silicate bioactive glasses (S53P4 and 45S5) leads to a decrease in the bioactivity. Metaphosphate bioactive glasses have been shown only to precipitate HA on remaining amorphous surfaces.

Regardless of the glass composition, partial to full crystallization leads to drastic change in the ions releasing rate and the dissolution mechanism. The dissolution behaviour of the crystallized phases is then different to that of the original glass. The crystallization of bioactive glasses is difficult to control, therefore leading to large variation from samples to sample disabling full prediction of the materials degradation.

The impact of glass crystallization on the bioactivity is dependent upon the crystals composition, size and density. Therefore, a better understanding of the crystallization mechanism of these glasses may allow for predictable ion release and enhanced mechanical properties.

Author details

Amy Nommeots-Nomm and Jonathan Massera*

*Address all correspondence to: jonathan.massera@tut.fi

BioMediTech Institute and Faculty of Biomedical Sciences and Engineering, Tampere University of Technology, Tampere, Finland

References

[1] O'Brien FJ. Biomaterials & scaffolds for tissue engineering. Materials Today. 2011;**14**:88-95. DOI: https://doi.org/10.1016/S1369-7021(11)70058-X

[2] Hench LL, et al. Bonding mechanisms at the interface of ceramic prosthetic materials. Journal of Biomedical Materials Research. 1971;**2**:117-141. DOI: 10.1002/jbm.820050611

[3] Fu Q, et al. Bioactive glass scaffolds for bone tissue engineering: State of the art and future perspectives. Materials Science and Engineering C: Materials for Biological Applications. 2010;**31**:1245-1256. DOI: https://doi.org/10.1016/j.msec.2011.04.022

[4] Hollinger JO, et al. Role of bone substitutes. Clinical Orthopaedics and Related Research. 1996;**324**:55-65

[5] Karageorgiou V, et al. Porosity of 3D biomaterial scaffolds and osteogenesis. Biomaterials. 2005;**26**:5474-5491. DOI: https://doi.org/10.1016/j.biomaterials.2005.02.002

[6] Gerhardt LC, Boccaccini AR. Bioactive glass and glass-ceramic scaffolds for bone tissue engineering. Materials. 2010;**3**:3867-3910. DOI: 10.3390/ma3073867

[7] Jones JR. Review of bioactive glass: From Hench to hybrids. Acta Biomaterialia. 2013;**9**(1): 4457-4486. DOI: http://dx.doi.org/10.1016/j.actbio.2012.08.023

[8] Deville S, Saiz E, Tomsia AP. Freeze casting of hydroxyapatite scaffolds for bone tissue engineering. Biomaterials. 2006;**27**(32):5480-5489. DOI: https://doi.org/10.1016/j.biomaterials.2006.06.028

[9] Huang TS, et al. Freeze extrusion fabrication of 13-93 bioactive glass scaffolds for repair and regeneration of load-bearing bones. Ceramic Transactions. 2011;**228**:45-55. DOI: 10.1007/s10856-011-4236-4

[10] Liu X, Rahaman MN, Fu Q. Oriented bioactive glass (13-93) scaffolds with controllable pore size by unidirectional freezing of camphene-based suspensions: Microstructure and mechanical response. Acta Biomaterialia. Acta Materialia Inc. 2011;**7**(1):406-416. DOI: 10.1016/j.actbio.2010.08.025

[11] Mallick KK. Freeze casting of porous bioactive glass and bioceramics. Journal of the American Ceramic Society. Blackwell Publishing Inc. 2009;**92**:S85-S94. DOI: 10.1111/j.1551-2916.2008.02784.x

[12] Chen QZ, Thompson ID, Boccaccini AR. 45S5 Bioglass®-derived glass-ceramic scaffolds for bone tissue engineering. Biomaterials. 2006;**27**(11):2414-2425. DOI: https://doi.org/10.1016/j.biomaterials.2005.11.025

[13] Fu Q, et al. Mechanical and in vitro performance of 13-93 bioactive glass scaffolds prepared by a polymer foam replication technique. Acta Biomaterialia. 2008;**4**(6):1854-1864. DOI: 10.1016/j.actbio.2008.04.019

[14] Hoppe A, et al. Cobalt-releasing 1393 bioactive glass-derived scaffolds for bone tissue engineering applications. ACS Applied Materials and Interfaces. 2014;**6**(4):2865-2877

[15] Sepulveda P, Binner JG. Processing of cellular ceramics by foaming and in situ polymerisation of organic monomers. Journal of the European Ceramic Society. 1999;**19**(12):2059-2066. DOI: 10.1016/S0955-2219(99)00024-2

[16] Wu ZY, et al. Melt-derived bioactive glass scaffolds produced by a gel-cast foaming technique. Acta Biomaterialia. Acta Materialia Inc. 2011;**7**(4):1807-1816. DOI: 10.1016/j.actbio.2010.11.041

[17] Vitale-Brovarone C, et al. Development of glass-ceramic scaffolds for bone tissue engineering: Characterisation, proliferation of human osteoblasts and nodule formation. Acta Biomaterialia. 2007;**3**(2):199-208. DOI: https://doi.org/http://dx.doi.org/10.1016/j.actbio.2006.07.012

[18] Desimone D, et al. Biosilicate(®)-gelatine bone scaffolds by the foam replica technique: Development and characterization. Science and Technology of Advanced Materials. 2013;**14**(4):45008. DOI: https://doi.org/10.1088/1468-6996/14/4/045008

[19] Baino F, Vitale-Brovarone C. Mechanical properties and reliability of glass-ceramic foam scaffolds for bone repair. Materials Letters. 2014;**118**:27-30. DOI: https://doi.org/http://dx.doi.org/10.1016/j.matlet.2013.12.037

[20] Chen Q, Mohn D, Stark WJ. Optimization of Bioglass® scaffold fabrication process. Journal of the American Ceramic Society. 2011;**94**(12):4184-4190. DOI: https://doi.org/10.1111/j.1551-2916.2011.04766.x

[21] Aguilar-Reyes EA, et al. Processing and in vitro bioactivity of high-strength 45S5 glass-ceramic scaffolds for bone regeneration. Ceramics International. 2017;**43**(9):6868-6875. DOI: https://doi.org/10.1016/j.ceramint.2017.02.107

[22] Wang H, et al. Three-dimensional zinc incorporated borosilicate bioactive glass scaffolds for rodent critical-sized calvarial defects repair and regeneration. Colloids and Surfaces B: Biointerfaces. 2015;**130**:149-156. DOI: https://doi.org/http://dx.doi.org/10.1016/j.colsurfb.2015.03.053

[23] Wang H, et al. Influence of Cu doping in borosilicate bioactive glass and the properties of its derived scaffolds. Materials Science and Engineering: C. 2016;**58**:194-203. DOI: https://doi.org/https://doi.org/10.1016/j.msec.2015.08.027

[24] Gu Y, et al. Bone regeneration in rat calvarial defects implanted with fibrous scaffolds composed of a mixture of silicate and borate bioactive glasses. Acta Biomaterialia. 2013;**9**(11):9126-9136. DOI: https://doi.org/10.1016/j.actbio.2013.06.039

[25] Fu H, et al. In vitro evaluation of borate-based bioactive glass scaffolds prepared by a polymer foam replication method. Materials Science and Engineering: C. 2009;**29**(7):2275-2281. DOI: http://doi.org/10.1016/j.msec.2009.05.013

[26] Nommeots-Nomm A, et al. Highly degradable porous melt-derived bioactive glass foam scaffolds for bone regeneration. Acta Biomaterialia. 2017;**57**:449-461. DOI: https://doi.org/10.1016/j.actbio.2017.04.030

[27] Fiocco L, et al. Bioactive wollastonite-diopside foams from preceramic polymers and reactive oxide fillers. Materials. 2015;**8**(5):2480-2494. DOI: 10.3390/ma8052480

[28] Kolan KCR, et al. Effect of material, process parameters, and simulated body fluids on mechanical properties of 13-93 bioactive glass porous constructs made by selective laser sintering. Journal of the Mechanical Behavior of Biomedical Materials. Elsevier. 2012;**13**:14-24. DOI: 10.1016/j.jmbbm.2012.04.001

[29] Velez M, et al. In vivo evaluation of 13-93 bioactive glass scaffolds made by selective laser sintering (SLS). In: Narayan R, Bose S, Bandyopadhyay A, editors. Biomaterials Science: Processing, Properties and Applications II. Hoboken, NJ, USA: John Wiley & Sons, Inc.; 2012. pp. 91-99. DOI: 10.1002/9781118511466.ch10

[30] Thavornyutikarn B, et al. Porous 45S5 Bioglass®-based scaffolds using stereolithography: Effect of partial pre-sintering on structural and mechanical properties of scaffolds. Materials Science and Engineering: C. 2017;**75**:1281-1288. DOI: https://doi.org/10.1016/j.msec.2017.03.001

[31] Cesarano III J, Segalman R, Calvert P. Robocasting provides moldless fabrication from slurry deposition. Ceramic Industry. 1998;148(4):94. Available from: https://ezp.lib.unimelb.edu.au/login?url=https://search.ebscohost.com/login.aspx?direct=true&db=edsggo&AN=edsgcl.20872588&site=eds-live&scope=site

[32] Fu Q, Saiz E, Tomsia AP. Direct ink writing of highly porous and strong glass scaffolds for load-bearing bone defects repair and regeneration. Acta Biomaterialia. 2011;**7**(10):3547-3554. DOI: 10.1016/j.actbio.2011.06.030.

[33] Cohn D, Sosnik A, Garty S. Smart hydrogels for in situ generated implants. Biomacromolecules. 2005;**6**(3):1168-1175. DOI: 10.1021/bm0495250

[34] Franco J, et al. Direct write assembly of calcium phosphate scaffolds using a water-based hydrogel. Acta Biomaterialia. Acta Materialia Inc. 2010;**6**(1):218-228. DOI: 10.1016/j.actbio.2009.06.031

[35] Lenaerts V, et al. Temperature-dependent rheological behavior of Pluronic F-127 aqueous solutions. International Journal of Pharmaceutics. 1987;**39**(1):121-127. DOI: http://dx.doi.org/10.1016/0378-5173(87)90206-7

[36] Grimal Q, et al. Assessment of cortical bone elasticity and strength: Mechanical testing and ultrasound provide complementary data. Medical Engineering & Physics. 2009;**31**(9):1140-1147. DOI: 10.1016/j.medengphy.2009.07.011

[37] Roohani-Esfahani S-I, Newman P, Zreiqat H. Design and fabrication of 3D printed scaffolds with a mechanical strength comparable to cortical bone to repair large bone defects. Scientific Reports. Nature Publishing Group. 2016;**6**(February 2015):19468. DOI: 10.1038/srep19468

[38] Deliormanli AM, Rahaman MN. Direct-write assembly of silicate and borate bioactive glass scaffolds for bone repair. Journal of the European Ceramic Society. Elsevier Ltd. 2012;**32**(14):3637-3646. DOI: 10.1016/j.jeurceramsoc.2012.05.005

[39] Liu X, et al. Mechanical properties of bioactive glass (13-93) scaffolds fabricated by robotic deposition for structural bone repair. Acta Biomaterialia. 2013;**9**(6):7025-7034. DOI: 10.1016/j.actbio.2013.02.026

[40] Eqtesadi S, et al. A simple recipe for direct writing complex 45S5 bioglass 3D scaffolds. Materials Letters. 2013;**93**:68-71. DOI: https://doi.org/10.1016/j.matlet.2012.11.043

[41] Eqtesadi S, et al. Robocasting of 45S5 bioactive glass scaffolds for bone tissue engineering. Journal of the European Ceramic Society. 2014;**34**(1):107-118. DOI: https://doi.org/10.1016/j.jeurceramsoc.2013.08.003

[42] Massera J, et al. Crystallization behavior of the commercial bioactive glasses 45S5 and S53P4. Journal of the American Ceramic Society. 2012;**95**:607-613. DOI: 10.1111/j.1551-2916.2011.05012.x

[43] Malek J, Mitsuhashi T. Testing method for the Johnson-Mehl-Avrami equation in kinetic analysis of crystallization processes. Journal of the American Ceramic Societies. 2000;**83**:2103

[44] Peitl Filho O, LaTorre GP, Hench LL. Effect of crystallization on apatite-layer formation of bioactive glass 45S5. Journal of Biomedical Research Part A. 1996;**30**:509-514. DOI: 10.1002/(SICI)1097-4636(199604)30:4<509

[45] Fagerlund S, et al. Phase composition and in vitro bioactivity of porous implants made of bioactive glass S53P4. Acta Biomaterialia. 2012;**8**:2331-2339. DOI: https://doi.org/10.1016/j.actbio.2012.03.011

[46] Ahmed I, et al. Processing, characterisation and biocompatibility of iron-phosphate glass fibres for tissue engineering. Biomaterials. 2004;**25**:3223-3232. DOI: https://doi.org/10.1016/j.biomaterials.2003.10.013

[47] Neel EAA, et al. Bioactive functional materials: A perspective on phosphate-based glasses. Journal of Materials Chemistry. 2009;**19**:690-701. DOI: 10.1039/B810675D

[48] Massera J, et al. Processing and characterization of novel borophosphate glasses and fibers for medical applications. Journal of Non-Crystalline Solids. 2015;**425**:52-60. DOI: 10.1016/j.jnoncrysol.2015.05.028

[49] Massera J, et al. The influence of SrO and CaO in silicate and phosphate bioactive glasses on human gingival fibroblasts. Journal of Materials Science: Materials in Medicine. 2015;**26**:196. DOI: 10.1007/s10856-015-5528-x

[50] Massera J, et al. Crystallization behavior of phosphate glasses and its impact on the glasses' bioactivity. Journal of Materials Science. 2015;**50**:3091-3102. DOI: 10.1007/s10853-015-8869-4

[51] Brink M. The influence of alkali and alkaline earths on the working range for bioactive glasses. Journal of Biomedical Research Part A. 1997;36:109-117. DOI: 10.1002/(SICI)1097-4636(199707)**36**:1<109

[52] Fu Q, et al. Silicate, borosilicate, and borate bioactive glass scaffolds with controllable degradation rate for bone tissue engineering applications. I. Preparation and in vitro degradation. Journal of Biomedical Research Part A. 2010;**95A**:164-171. DOI: 10.1002/jbm.a.32824

[53] Fabert M, et al. Crystallization and sintering of borosilicate bioactive glasses for application in tissue engineering. Journal of Materials Chemistry B. 2017;**5**:4514-4525. Available online. DOI: 10.1039/C7TB00106A

INTECH

INTECH